ELSEVIER

Catalysis Today 40 (1998) 229–243

CATALYSIS TODAY

Reducibility of undoped and Cs-doped α-$NiMoO_4$ catalysts: Kinetic effects in the oxidative dehydrogenation of *n*-butane

L.M. Madeira[a], M.F. Portela[a,*], C. Mazzocchia[b], A. Kaddouri[b], R. Anouchinsky[b]

[a] *GRECAT- Grupo de Estudos de Catálise Heterogénea. Instituto Superior Técnico-Universidade Técnica de Lisboa. Av. Rovisco Pais, 1096 Lisbon Codex, Portugal*

[b] *Dipartimento di Chimica Industriale ed Ingegneria Chimica. Politecnico de Milano. 32 P.za L. Da Vinci, 20133 Milan, Italy*

Abstract

Temperature-programmed reduction (TPR) was used to study the reduction of undoped and doped α-$NiMoO_4$ with several Cs loads. The results contributed to clarify the mechanism of the nickel molybdate reduction by hydrogen. It was found that the reducibility of the catalysts, as inferred from the temperature of reduction onset, decreases with Cs load. The catalysts were tested for the oxidative dehydrogenation of *n*-butane and the activity followed the same trend recorded in the TPR experiments. It was possible to conclude that the catalytic activity is related to the reducibility of the sample while the selectivity is determined by the basicity of the surface. Kinetic studies over unpromoted and 3% Cs-promoted α-$NiMoO_4$ evidenced that Cs doping only affects the partial order with respect to butane, which i ncreases for dehydrogenation products and decreases for CO and CO_2. The partial order with respect to oxygen is almost unaffected. The kinetic results were discussed based on the basicity and reducibility of the catalysts. © 1998 Elsevier Science B.V.

Keywords: Nickel molybdate; Cesium doping; Reduction; Butane oxidative dehydrogenation; Kinetics

1. Introduction

Molybdenum-based oxides are versatile catalysts for important industrial processes. In particular, nickel molybdenum oxides are used for several reactions such as hydrodesulphurization [1,2], partial oxidation of hydrocarbons [3–5] and oxidative dehydrogenation (ODH) of alkanes [6,7].

In a previous study we have shown, either by changing the nature or the concentration of the promoter, that alkali promoters affect the catalytic behaviour of both α and β-phases of nickel molybdate in *n*-butane ODH [8]. In particular, cesium addition was found to increase significantly the selectivity to dehydrogenation products [9].

It is well known that the catalytic behaviour of a catalyst in selective oxidation reactions is related to its redox properties. Several papers have made references to very interesting correlations between the reducibility of catalysts and the catalytic behaviour in selective butane oxidation [10–13].

Temperature-programmed reduction (TPR) experiments can provide valuable insight into the role of the reduction properties. In this way, it was found interesting to study both, the process of $NiMoO_4$ reduction,

*Corresponding author.

PII S0920-5861(98)00011-X

which has not yet been unambiguously established in spite of the number of reports found in literature [1,14–16], and the effects of cesium promotion on such properties. Finally, it will be attempted to relate the effects of Cs addition to $NiMoO_4$ on the kinetics of *n*-butane ODH with the reducibility of the catalysts.

2. Experimental

2.1. Catalysts preparation and characterization

The stoichiometric $NiMoO_4$ was prepared by coprecipitation reaction, following the method described by Mazzocchia et al. [3], using 0.25 M solutions of $Ni(NO_3)_2{\cdot}6H_2O$ and H_2MoO_4. Cs-doped catalysts were prepared by wet impregnation of the pure α-$NiMoO_4$ with a solution of cesium nitrate at 60°C for 15 h. The impregnated solids were then filtered, dried at 120°C and, finally, calcined in air at 550°C for 2 h. The Cs-doped samples were labelled *x*Cs–$NiMoO_4$, in which *x* denotes the surface atomic ratio Cs/Mo (%), determined by XPS [9].

The characterization of the samples was performed by using several techniques: ICP, AA, BET, HTXRD, FTIR, CO_2-TPD and XPS. Experimental details and results can be found elsewhere [8,9]. X-ray diffractograms were obtained at room temperature in a Philips PW 1130 X-ray generator with CuK_α radiation (Ni filter).

2.2. Temperature-programmed reduction

Before the runs, a pre-treatment was performed by heating the sample (50 mg) in argon flow (50 ml/min) up to 150°C and maintaining this temperature for 60 min. Then the quartz reactor containing the sample was cooled to room temperature and a mixture of 5% hydrogen in argon (60 ml/min), purified with an oxy-trap and molecular sieves, was used to reduce the catalyst by heating at 10°C/min up to the desired temperature. A blank run proved that when the sample was heated in argon flow up to 800°C the detector signal was negligible. On-line gas analysis was performed with a thermal conductivity detector. A solid CO_2 trap set after the reactor removed the water formed during reaction. Thus, the detector response was only proportional to H_2 consumption.

The amount of H_2 consumed in the runs was quantified by the peak-area integration method. NiO, prepared by calcination of nickel nitrate hexahydrate (Fluka Chemika, p.a.) for 2 h at 550°C in air flow, was used to calibrate the TCD response. The accuracy of the measurements was cross-checked by comparing results of several TPR runs and it was found to be better than 5%.

2.3. Catalytic tests

Catalytic runs were performed in a fixed-bed continuous-flow quartz tubular reactor with a coaxially centred thermocouple. Reactants and products were analyzed with an on-line Shimadzu GC-8A gas chromatograph with two columns as described elsewhere [8,9].

The catalyst was mixed with inert quartz (50–70 mesh) in a catalyst-to-quartz volume ratio of 1 : 2. The catalyst charge was chosen to yield differential conversions minimizing the effects of products and secondary reactions. It was intended to have conversions less than 5% for butane. In case of oxygen, preliminary experiments showed that it was not required to be so strict. The feed was a mixture of *n*-butane, oxygen and nitrogen and the total pressure in the reactor was 1.10 bar. For comparisons based on equal conversion levels, the temperature was adjusted to maintain constant conversion of butane.

In the kinetic studies with unpromoted, and 3% Cs promoted α-$NiMoO_4$, temperatures used were 500, 520, 540 and 560°C. In both cases, the influence of the reactants partial pressure was studied by fixing P_{butane} at 0.05 bar and by varying P_{O_2} from 0.02 to 0.15 bar. With unpromoted $NiMoO_4$, the butane partial pressure was changed from 0.02 to 0.10 bar (with P_{O_2} = 0.05 bar) and from 0.05 to 0.15 bar (with P_{O_2} = 0.15 bar). The catalyst charge was 0.150 g and the contact time (*W*/*F*) 4.45 g h/mol_{butane}. With the Cs-promoted catalyst, the butane partial pressure was changed from 0.02 to 0.25 bar (with P_{O_2} = 0.05 bar). bar). The catalyst charge was 0.300 g and *W*/*F*= 5.80 g h/mol_{butane} [17].

Blank runs proved that under the experimental conditions used the homogeneous reactions can be neglected.

3. Results and discussion

3.1. Catalysts characterization

Extensive characterization of the catalysts, concerning the $NiMoO_4$ purity and the effects of Cs addition, was previously described [8,9]. It was shown that Cs is deposited only on the catalyst surface and does not affect the bulk. In this way, some properties of the catalyst surface were affected. In fact, a decrease of the catalyst surface area was observed on increasing the Cs content. The binding energies of Mo_{3d} XPS spectra also decrease, suggesting an increase of the average electron density of the molybdenum atoms. Finally, CO_2-TPD experiments showed that Cs doping leads to an increase in the catalyst basicity with respect to the unpromoted $NiMoO_4$, as would be expected according to the electron-donor character of such promoter.

3.2. Temperature-programmed reduction

Fig. 1 shows the TPR spectrum of nickel oxide used as standard in order to quantify the amount of H_2 consumed in the experiments by peak-area integration method. The spectrum agrees very well with that found in the literature [14]. The TPR profile exhibits a single peak at 390°C corresponding to the reduction to metallic nickel. In fact, the X-ray diffraction pattern of the calcined nickel nitrate presented in Fig. 2(A) corresponds to pure nickel oxide (JCPDS card 4-0835) and only metallic Ni was found after reduction up to 675°C (Fig. 2(B)).

3.2.1. Pure α-$NiMoO_4$

The shape of the $NiMoO_4$ TPR profile (Fig. 3(A)) is similar to those already published [1,14–16], showing two maxima at 545 and 725°C, respectively. The first one is usually broad and with a certain asymmetry in the low-temperature side. It is well known that, besides the different experimental conditions (e.g. heating rates), the position of the peaks is affected by several factors such as small variations in the composition of the samples inside the homogeneity domain, crystallite size, ageing of the samples, state of hydration or chemical interactions between the different species [14]. Brito et al. [1], using experimental conditions very similar to those described above, found two maxima at 575 and 730°C, respectively.

The compositions of the products from $NiMoO_4$ reduction have not been established unambiguously. In Table 1, some mechanisms proposed in the literature for reduction of the Ni–Mo–O system are summarized. Evidently, the intermediates as well the final products of complete reduction differ with the authors. For clarifying the situation, a study of the $NiMoO_4$ reduction process was performed, with the main objective of identifying the reduction products. In this sense, XRD analysis were performed after interruption of the TPR runs at selected temperatures and

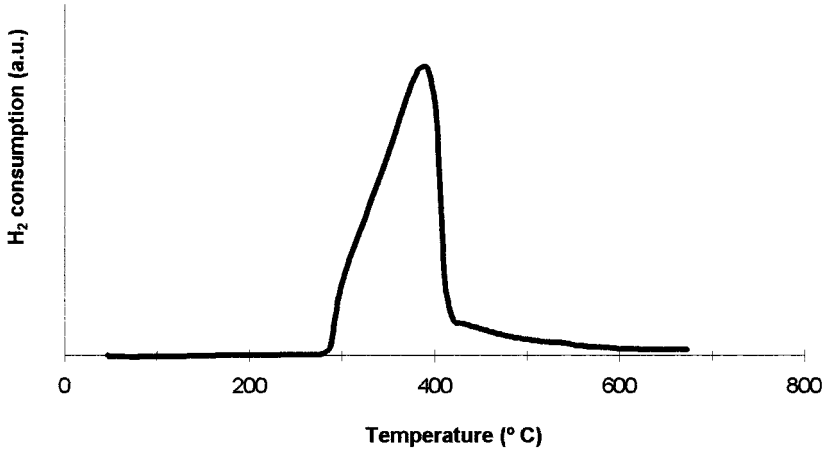

Fig. 1. TPR profile of NiO used as standard (W=50 mg).

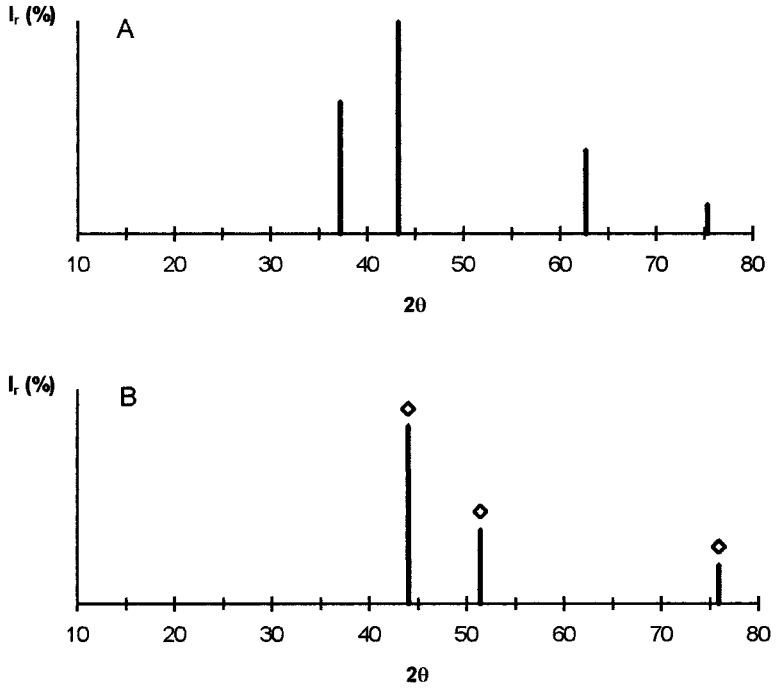

Fig. 2. XRD patterns of (A) fresh NiO and (B) NiO after reduction on H_2 up to 675°C. ◇, Metallic Ni.

Table 1
Mechanisms and intermediate products of $NiMoO_4$ reduction by hydrogen

	1st step			2nd step		Reference
$NiMoO_4$	$\rightarrow^{(475°C)}$	Ni + Ni–Mo alloys + MoO_2 + intermetallics (e.g. Ni_4Mo)	MoO_2	$\rightarrow^{(700°C)}$	Mo	[14]
$NiMoO_4$	$\rightarrow^{(400-500°C)}$	Ni–Mo alloy + amorphous molybdenum lower oxide	amorphous molybdenum lower oxide phase	$\rightarrow^{N_2(600°C)}$	MoO_2	[18]
$NiMoO_4$	$\rightarrow^{(300-450°C)}$	Ni+MoO_2				[19,20]
$NiMoO_4$	$\rightarrow^{(300-500°C)}$	$NiMo_x$ alloy+MoO_2	$NiMo_x$ alloy+MoO_2	$\rightarrow^{(700°C)}$	Mo+Ni_3Mo	[16]
$NiMoO_4$	$\rightarrow^{(500-600°C)}$	Ni+Mo_2O_3	Ni+Mo_2O_3		intermetallide of Ni and Mo	[21]

cooling the samples to room temperature. The selected temperatures were those corresponding to the maxima in the TPR profile (545 and 725°C), the minimum between them (at 620°C) and the final temperature of the runs (800°C). In Fig. 4, the recorded X-ray diffraction patterns are presented, including the fresh $NiMoO_4$, which corresponds to the pure α-molybdate (JCPDS card 33-948).

The hydrogen consumption begins only at 300°C (Fig. 3(A)) and at 545°C the X-ray diffractogram (Fig. 4(B)) shows only three broad peaks. These peaks are probably due to metallic nickel and/or to the intermetallic Ni_4Mo (JCPDS cards 4-850 and 3-1036, respectively) whose characteristic lines are almost coincident. The formation of the intermetallic (d=2.052 Å) was already reported by Brito et al. [14], whereas Tsigdinos and Swanson [22] had stated that such a compound can be a reduction product of anhydrous nickel molybdate.

When the reduction was performed up to 620°C (Fig. 4(C)), new peaks appeared, characteristic of MoO_2 (JCPDS card 5-452). This phase was found

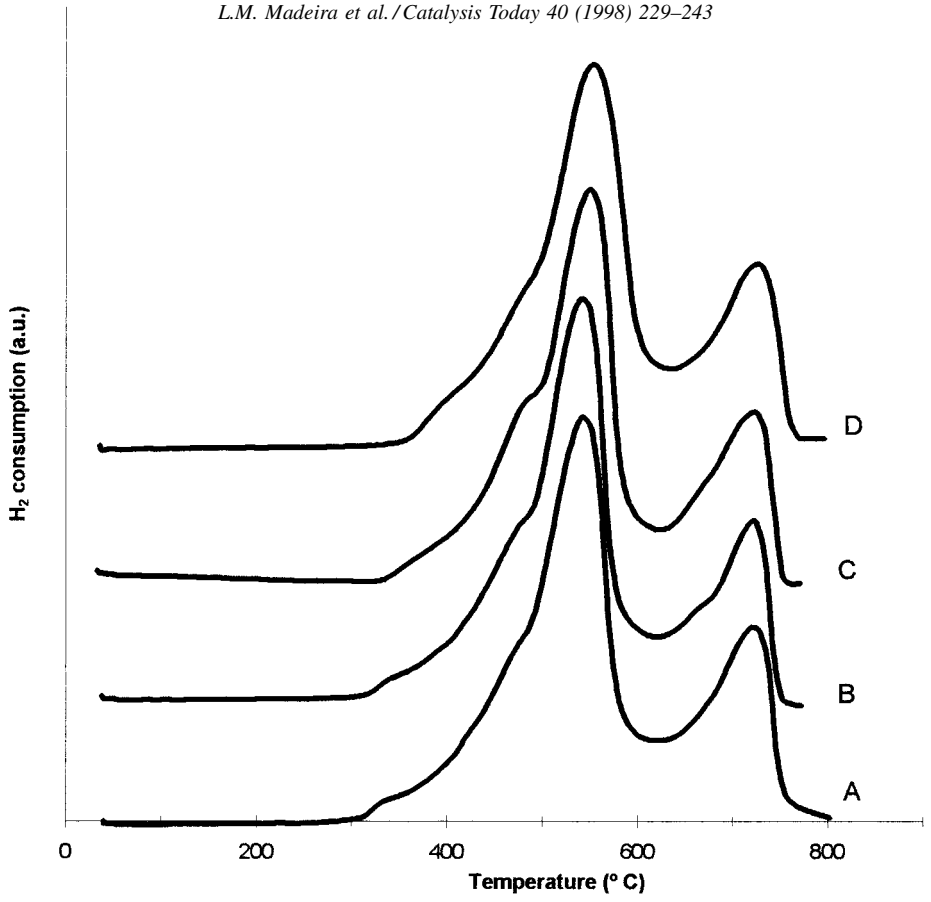

Fig. 3. TPR profiles of unpromoted (A) and Cs-promoted α-$NiMoO_4$ 1% Cs (B); 3% Cs (C) and 6% Cs (D).

in almost all the works concerning the $NiMoO_4$ reduction. However, some authors found an amorphous material. According to Brito et al. [14], reduction of MoO_3 to MoO_2 under the dynamic conditions of TPR proceeds with the formation of a highly amorphous or 'porous' oxide. Moreover, Kipnis and Agievskii [18] proposed (cf. Table 1) that the reduction of nickel molybdate by H_2 at 400–500°C leads to the formation of an Ni–Mo alloy and a finely dispersed lower Mo oxide phase that crystallizes as MoO_2 when heated at 600°C. These facts explain the broadness of the peaks in the X-ray diffractograms and the absence of the MoO_2 characteristic lines in Fig. 4(B).

The reduction of the $NiMoO_4$ sample up to the temperature of the second maximum (Fig. 4(D)) shows the existence of other phases: metallic Mo (JCPDS card 4-809), an Ni–Mo alloy and a small amount of intermetallic Ni_3Mo (JCPDS card 17-572). When the temperature is increased up to 800°C, the quantity of such a compound becomes more significant (Fig. 4(E)), with detriment of the alloy. The Ni–Mo alloy, which is probably enriched in Ni, has been already found by other authors (cf. Table 1) and presents two characteristic lines in the X-ray pattern located at ca. 2.070 and 1.789 Å, respectively.

3.2.2. *Cs-promoted α-$NiMoO_4$*

The TPR profile is almost unaffected by addition of Cs to the catalyst (Fig. 3(B–D)), i.e. the amount of hydrogen consumption (defined by the area of the curve) is the same for unpromoted and promoted $NiMoO_4$, showing that the extent of reduction was not significantly affected by Cs presence. Quantification of the amount of H_2 consumed in the runs shows that, within an experimental error of ca. 15%, the oxides are completely reduced to the metallic state

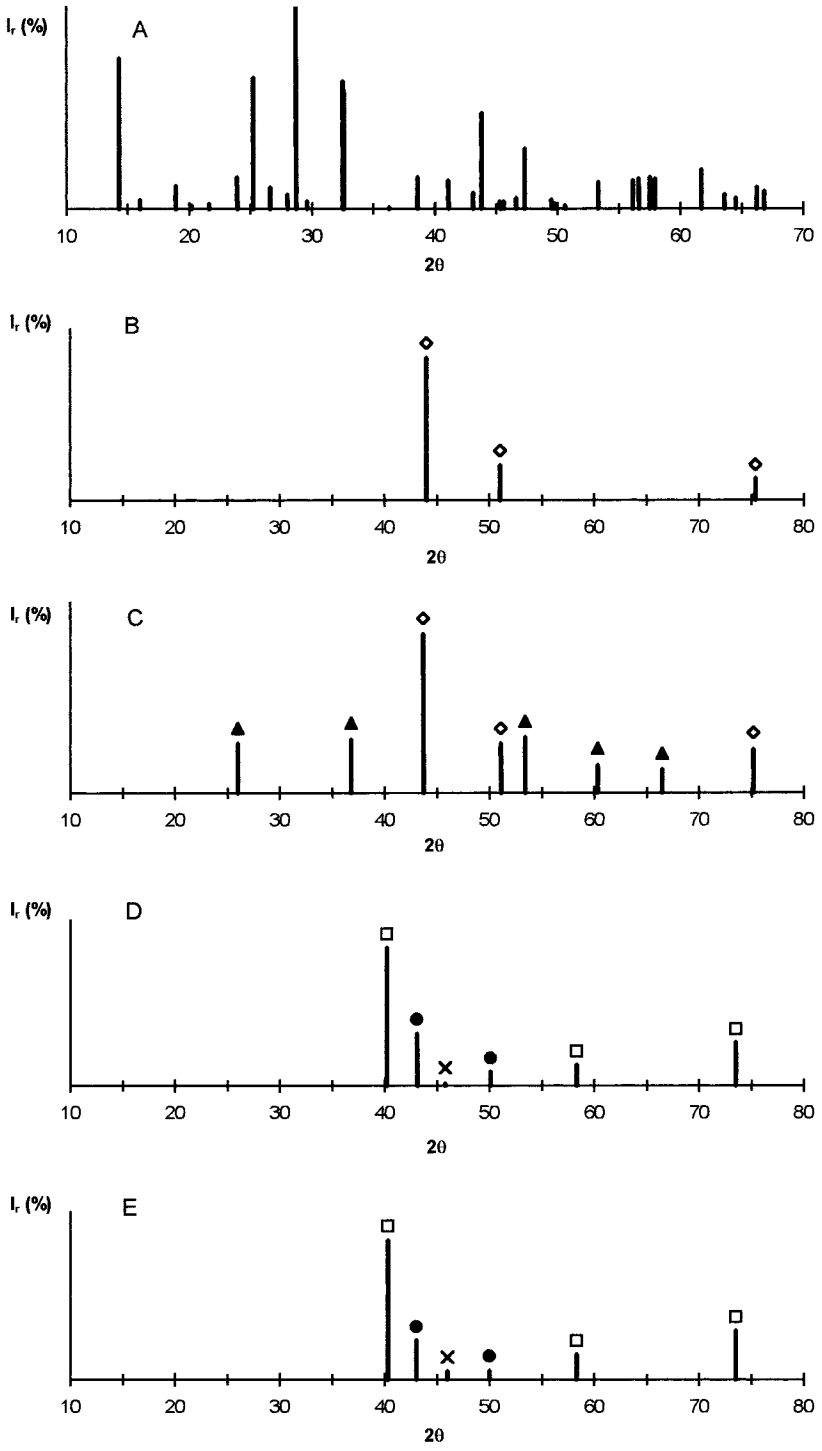

Fig. 4. XRD patterns of fresh α-$NiMoO_4$ (A) and after reduction on H_2 up to different temperatures: 545°C (B); 620°C (C); 725°C (D); and 800°C (E). ◇, Metallic Ni and/or intermetallic Ni_4Mo; ▲, MoO_2; □, metallic Mo; ●, Ni–Mo alloy; and ×, intermetallic Ni_3Mo.

Table 2
TPR data of catalyst samples

Catalyst	T_{onset} [a]	T_{m_1} [b]	T_{m_2} [c]	H_2 consumption (mmol/g_{cat})		
	(°C)	(°C)	(°C)	1st peak	2nd peak	Total
$NiMoO_4$	300	545	725	11.6	4.1	15.7
1% Cs–$NiMoO_4$	320	545	725	11.5	4.0	15.5
3% Cs–$NiMoO_4$	335	550	725	11.0	3.8	14.8
6% Cs–$NiMoO_4$	350	555	725	11.6	4.0	15.6

[a] Temperature of onset of reduction.
[b] Temperature of the first peak maximum.
[c] Temperature of the second peak maximum.

(Table 2). Moreover, X-ray diffraction patterns of all the reduced samples were the same, showing only the presence of metallic molybdenum, Ni_3Mo intermetallic and an Ni–Mo alloy after reduction up to 800°C. The extent of the reduction after the first TPR peak amounts to 74% of the total H_2 consumption, and is interpreted, in agreement with the previous discussion to formation of metallic nickel or intermetallic compounds (such as Ni_4Mo) dispersed on MoO_2. The latter is further reduced to metallic Mo under the second TPR peak, accompanied by the formation of an Ni–Mo alloy and Ni_3Mo.

As mentioned above, the TPR profiles were similar for all the four catalysts. However, there are some changes in the temperature of reduction onset and in maxima temperatures (Table 2). The temperature of the second maximum was not affected by Cs presence and it is 725°C for all samples, whereas the temperature of the first maximum increased slightly. However, a significant increase for the onset of temperature of reduction was recorded on increasing Cs contents. These results show that although Cs promotion does not affect the global consumption of H_2, it increases the reduction resistance of the nickel molybdate. The increase of 50°C in T_{onset} must be pointed out for such a small amount of promoter in the catalyst, i.e. a surface concentration of Cs with respect to Mo (atomic ratio) of 6%. Similar effects by Li, Na and K doping over molybdate catalysts were found by Driscoll et al. [23] and by Cs doping over vanadium oxide catalysts by Owens and Kung [10].

3.3. Catalytic tests

Previous reaction studies based on the effects of alkali metal promoters on nickel molybdate catalysts [8] and specially when increasing the cesium content [9], showed that the addition of such promoters generally reduces the catalytic activity for ODH of butane, but yields higher selectivities to butenes and butadiene (C_4's). This behaviour was related with the physical and chemical effects of Cs doping mentioned above. In Table 3 the rates of butane conversion at 475°C and the selectivity to dehydrogenation products, found for

Table 3
Catalytic results in butane ODH over unpromoted and Cs promoted α-$NiMoO_4$ [a]

Catalyst (S_{BET} (m^2/g))	r_{butane} [b]$\times 10^3$ (mol/(h g))	r_{butane} [b]$\times 10^5$ (mol/(h m^2))	S_{C_4}'s [c] (%)	$T_{5\%}$ [d] (°C)
$NiMoO_4$ (44.1)	8.9	20.1	53.7	425
1% Cs–$NiMoO_4$ (34.9)	2.5	7.1	81.5	500
3% Cs–$NiMoO_4$ (28.7)	1.4	5.0	86.5	525
6% Cs–$NiMoO_4$ (26.7)	1.0	3.7	61.6	550

[a] Feed: 4% butane; 9% O_2; 87% N_2; W/F=12 g h/mol_{butane}; and W=0.300 g.
[b] Rates of butane conversion at 475°C.
[c] Selectivity to butenes and butadiene at conversion level of 5%.
[d] Temperature at which the butane conversion level is 5%.

all the studied catalysts, are shown. The decrease in butane conversion by Cs addition is not only due to the decrease in the surface area, because when rates of butane conversion are based on unity surface area the trend is the same. With respect to selectivity, the C_4 formation is favoured by Cs presence although in the case of 6% Cs–$NiMoO_4$ an overdoping effect detected by CO_2-TPD measurements [9] leads to an increase of the CO_x selectivity. Basicity was found to be fundamental to promote the selective ODH of butane, because in this way, butenes and butadiene interact more weakly with the catalyst surface, decreasing the chances of being overoxidized.

To compare the selectivity to dehydrogenation products at isoconversion, temperature was adjusted for each catalyst (Table 3). As expected, there is an increase of reaction temperature when the Cs content is increased because the catalysts are progressively less active. It is noteworthy that the largest increase in reaction temperature is observed from the unpromoted catalyst to 1% Cs-doped $NiMoO_4$. The observed selectivity for the 6% Cs sample can also be due to the high temperature necessary to compensate the loss of activity. But this would not be the only reason for such strong decrease. In fact, from the unpromoted catalyst to the 3% Cs-doped $NiMoO_4$, there is an increase of 100°C in the reaction temperature to keep the butane conversion constant. However, in such circumstances selectivity to dehydrogenation products is largely improved. For the 6% Cs sample, an increase of only 25°C leads to a strong decrease in selectivity with respect to the 3% Cs–$NiMoO_4$ catalyst. In this way, such behaviour would be mainly due to a decrease in basicity.

To understand certain fundamental aspects of the mechanism of reaction, a systematic kinetic study over the unpromoted and Cs-doped α-$NiMoO_4$ catalysts was performed. The effects of Cs in the kinetics of *n*-butane ODH was studied using the most selective catalyst, namely 3% Cs–$NiMoO_4$ [17].

The products found in the conversion of *n*-butane over unpromoted and Cs-promoted α-$NiMoO_4$ catalysts were carbon oxides (CO and CO_2) and products of selective dehydrogenation (C_4's): 1-butene, 2-*trans*-butene, 2-*cis*-butene and butadiene.

The influence of the partial pressure of the reactants and temperature was studied for unpromoted α-$NiMoO_4$. First, the butane partial pressure was fixed at 0.05 bar and P_{O_2} varied from 0.02 to 0.15 bar. Then, the oxygen partial pressure was maintained at 0.05 bar and P_{butane} changed from 0.02 to 0.10 bar. Due to the catalyst reduction and/or coke formation, it was not possible to work with higher butane concentrations (with $P_{O_2} = 0.05$ bar). In this way, we made some more tests with $P_{O_2} = 0.15$ bar, varying P_{butane} from 0.05 to 0.15 bar. Again, catalyst reduction and/or coke formation was observed at higher butane concentrations. In Figs. 5–8, the experimental rates based on surface area for the unpromoted α-phase are presented.

The ODH of *n*-butane was also carried out over the most selective catalyst: 3% Cs–$NiMoO_4$ [17] over a wide range of experimental conditions (temperature, contact time and partial pressure of both butane and oxygen). While the formation rates of CO_x are almost independent of the butane partial pressure (P_{butane}), especially CO_2, the selective dehydrogenation rates are independent of the partial pressure of oxygen (P_{O_2}). Moreover, the formation rates for both 2-butenes increase linearly with P_{butane} while this increase presents a decreasing slope in the case of 1-butene and butadiene. It is noteworthy that, in the kinetic study with 3% Cs–$NiMoO_4$, we worked with butane partial pressures up to 0.25 bar (with $P_{O_2} = 0.05$ bar) without reduction of the catalyst or coke formation.

For both catalysts, the experimental rates (r_i) were fitted to power-law rate equations [Eq. (1)] by non-linear regression analysis with a multiple correlation coefficient ψ [24,25]:

$$r_i = k P_{butane}^{n_1} P_{O_2}^{n_2} \quad (1)$$

where k is a kinetic constant that shows Arrhenius behaviour:

$$k = k_0 \exp(-E_a/RT) \quad (2)$$

The obtained values for the parameters are presented in Table 4. Reasonable fittings were found except for CO_x, especially CO, with the Cs-doped $NiMoO_4$. The poor correlation coefficients in these cases reflect the dispersion of experimental data with respect to P_{O_2} [17] because ψ is very sensitive to such dispersion.

The lines of Figs. 5–8 correspond to the fitting curves obtained by Eq. (1) with the computed parameters. Fig. 5 shows that the butane consumption rates exhibit a similar dependence on oxygen and

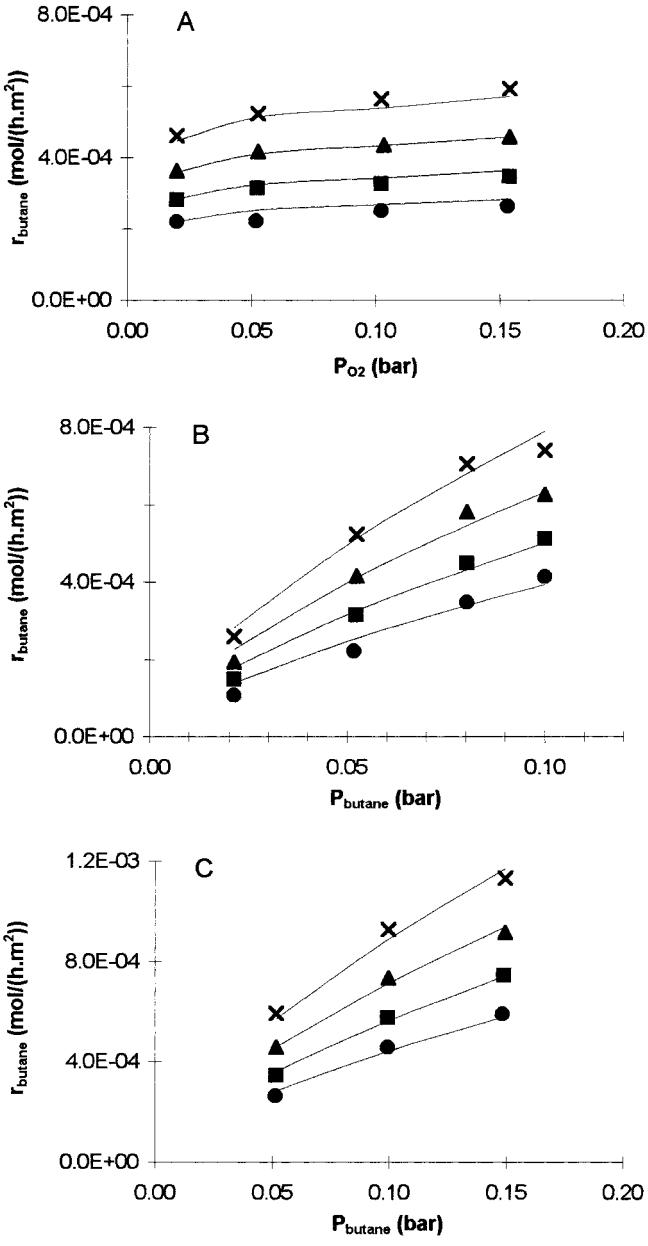

Fig. 5. Influence of oxygen partial pressure (P_{O_2}) variation at (A) butane partial pressure (P_{butane})=0.05 bar and P_{butane} variation at (B) P_{O_2} = 0.05 bar and (C) 0.15 bar on the butane conversion rates over α-$NiMoO_4$. ●, 500°C; ■, 520°C; ▲, 540°C; and ×, 560°C.

butane concentrations as in the case of 3% Cs–$NiMoO_4$, i.e. increase with both P_{butane} and P_{O_2} but, in the last case the dependence is much smaller (partial orders of 0.67 and 0.11, respectively).

Fig. 6 evidences that CO and CO_2 formation rates present very similar dependence on the partial pressures of the reactants, increasing with both P_{butane} and P_{O_2}, specially with butane concentrations. It is noteworthy that when using the 3% Cs-$NiMoO_4$ catalyst, CO_2 formation rates and CO formation rates at the lower temperatures are independent of P_{butane}, but tend to increase with P_{O_2} [17]. The formation rates

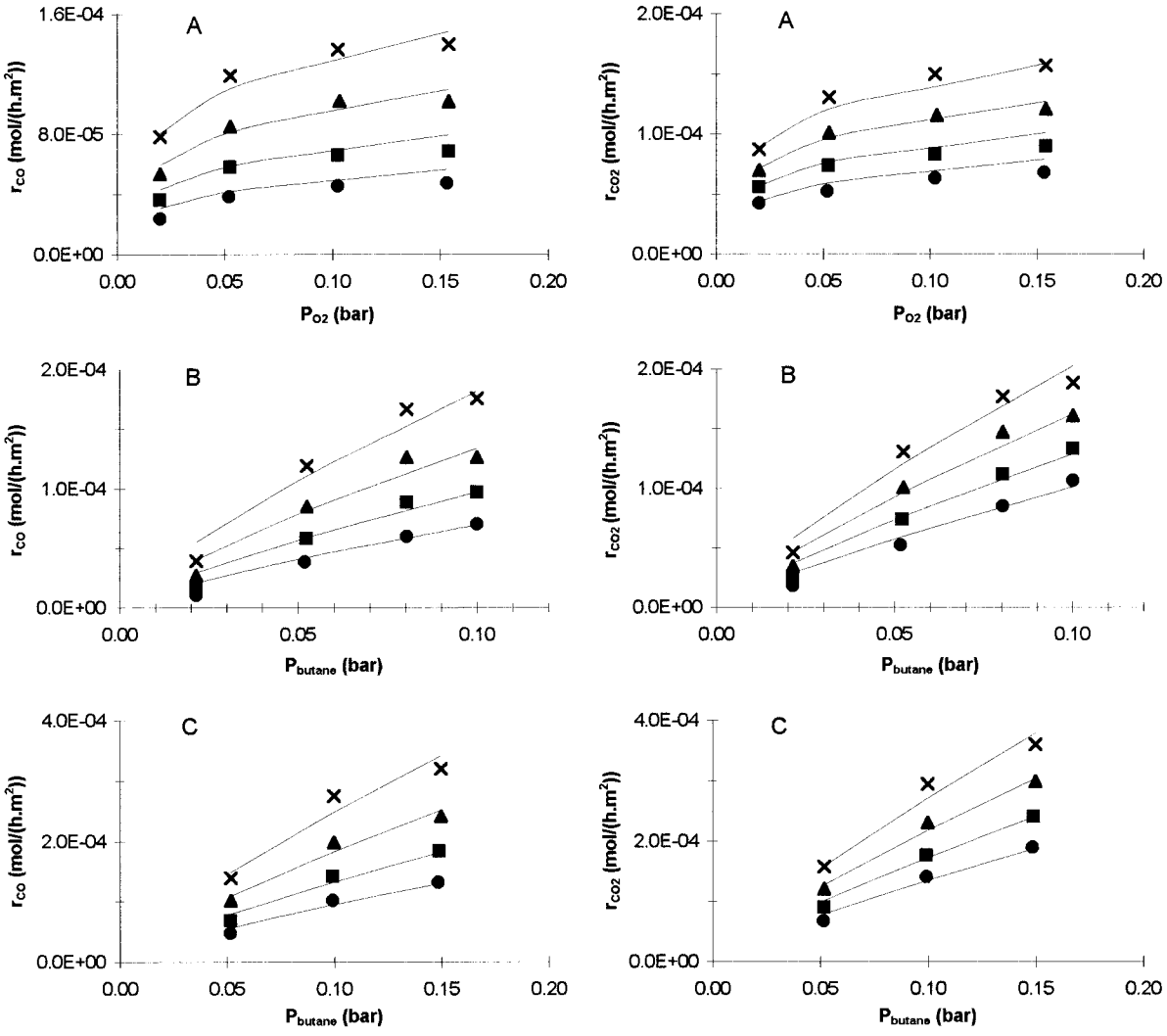

Fig. 6. Influence of P_{O_2} and P_{butane} on CO and CO_2 formation rates over α-$NiMoO_4$. Operating conditions and symbols as in Fig. 5.

of the dehydrogenation products (Figs. 7 and 8) also increase with P_{butane} but are independent of P_{O_2}. As in the case with the Cs-promoted sample, the dehydrogenation processes do not appear to be influenced by the gaseous oxygen.

From the results in Table 4 it is clear that the activation energies for all product formation, or butane consumption, over the 500–560°C range, are higher for the Cs-doped catalyst. Within experimental uncertainties, the partial order with respect to oxygen for any product is maintained after the addition of Cs. However, Cs doping provokes an increase of the partial order with respect to butane for the dehydrogenation products and a decrease for CO_x formation. These effects of Cs doping result from the catalytic data mentioned before, i.e. a decrease in the nickel molybdate activity for butane conversion but an increase in the selectivity for C_4 formation.

Finally, it should be remarked that the partial orders with respect to butane and oxygen for butane conversion are not significantly affected by the dopage (cf. Table 4), suggesting that this promoter affects both the rates of reduction and reoxidation of the catalyst to the

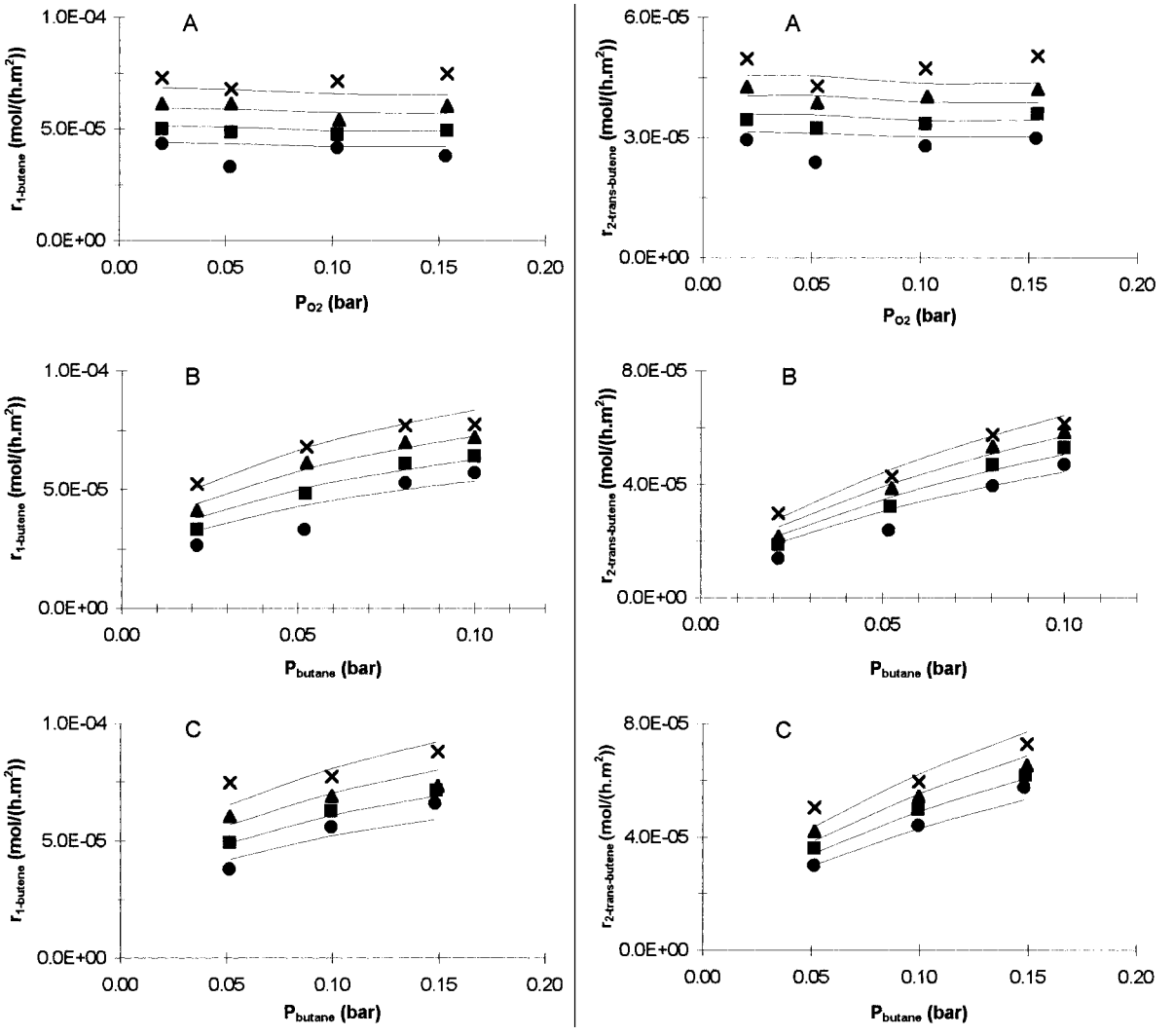

Fig. 7. Influence of P_{O_2} and P_{butane} on the 1-butene and 2-*trans*-butene formation rates over α-$NiMoO_4$. Operating conditions and symbols as in Fig. 5.

same extent, resulting in slight changes in the overall kinetics.

4. Conclusions

TPR is a fast and good technique to complement other techniques for the characterization of catalysts involved in reactions with possible redox type mechanisms.

The results obtained when stopping TPR experiments at convenient temperatures and analyzing reduction products by XRD, made it possible to understand the mechanism of the $NiMoO_4$ reduction with H_2, which is summarised in Scheme 1.

The nickel molybdate reduction starts at fairly low temperatures (300°C), leading to metals (Ni and probably Ni_4Mo) and amorphous MoO_2. Ni^{2+}, after being reduced to metallic nickel, activates molecular hydrogen, promoting the reduction of Mo^{6+}. The

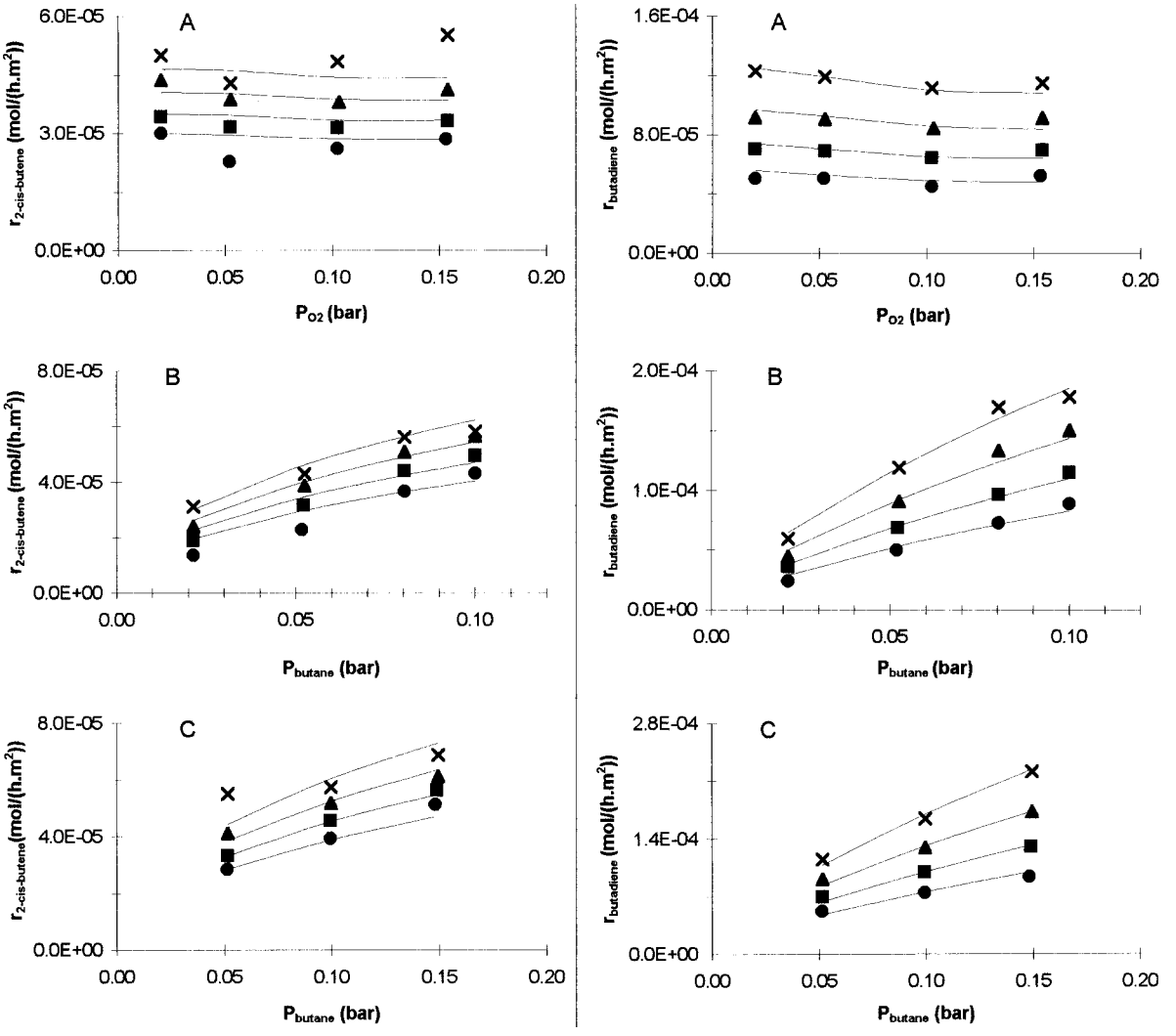

Fig. 8. Influence of P_{O_2} and P_{butane} on the 2-*cis*-butene and butadiene formation rates over α-$NiMoO_4$. Operating conditions and symbols as in Fig. 5.

amount of formed MoO_2 is only significant at ca. 620°C. In this way, the low-temperature peak may be assigned to the reduction of all Ni^{2+} to metallic nickel and of the Mo^{6+} to Mo^{4+} or to the metallic state. The second TPR peak would be concerned with reduction of Mo^{4+}. Metallic nickel acts as a hydrogen activator and induces reduction of molybdenum with the formation of metallic Mo and an Ni–Mo alloy. Finally, at temperatures >725°C, a mixture of Mo, Ni–Mo alloy and Ni_3Mo intermetallic was found.

TPR measurements have also been performed with doped $NiMoO_4$ using different cesium loads (1, 3 and 6%). It was found that the global hydrogen consumption is practically unaffected by the dopage as well as the temperature of the second peak maximum (725°C for all the samples) and only a slight increase in the temperature of first peak maximum was recorded (from 545°C for unpromoted $NiMoO_4$ to 555°C for 6% Cs–$NiMoO_4$). However, the temperature of onset of reduction increased significantly with increasing Cs

Table 4
Computed parameters by fitting Eq. (1) to the experimental rates

Catalyst		1-butene	2-*trans*-butene	2-*cis*-butene	Butadiene	CO	CO_2	Butane
$NiMoO_4$	k_0 (mol/(h m^2))	4.8×10^{-2}	2.4×10^{-2}	4.9×10^{-2}	23	630	24	42
	E_a (kJ/mol)	39.4	33.0	39.2	72.1	85.8	62.3	62.3
	n_1	0.32	0.54	0.47	0.68	0.79	0.82	0.67
	n_2	−0.03	−0.03	−0.03	−0.08	0.29	0.27	0.11
	ψ	0.92	0.95	0.93	0.99	0.98	0.99	0.99
3% Cs–$NiMoO_4$	k_0 (mol/(h m^2))	44	7	11	3209	1.5×10^{7}	369	1272
	E_a (kJ/mol)	75.9	64.5	66.2	104.9	171.4	99.9	88.0
	n_1	0.78	0.95	1.03	0.76	0.43	−0.03	0.70
	n_2	0.06	0.05	0.01	0.08	0.33	0.38	0.16
	ψ	0.99	0.99	1.00	0.97	0.84	0.92	0.99

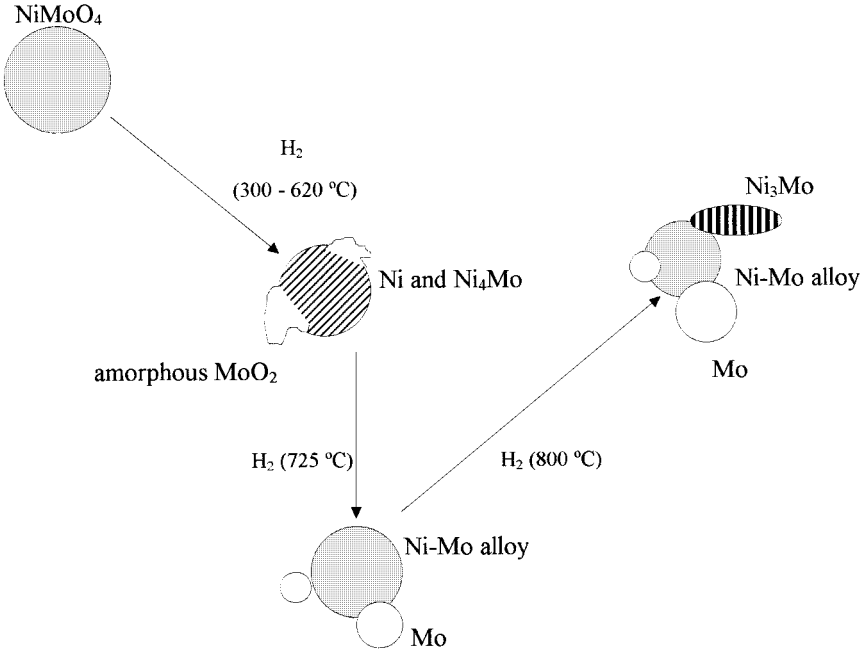

Scheme 1. Phase composition of the products from $NiMoO_4$ reduction.

load (from 300°C for unpromoted $NiMoO_4$ to 350°C for 6% Cs–$NiMoO_4$). This means that the promoter increases resistance of the catalyst to reduction. Increased resistance to reduction by hydrocarbons due to alkali metal doping has also been reported by other authors [26].

Catalytic tests showed that Cs addition leads to lower activity for butane conversion but gives higher dehydrogenation selectivities. Similar results were obtained by Owens and Kung after Cs modification of unsupported vanadium oxide catalysts for butane oxidation [10] and it was also reported that modification of a catalyst, resulting in an increase of resistance to reduction, induces higher selectivities in butane oxidation [10–12,26]. According to Kung [27], there is a relationship between the reducibility of the catalysts and the selectivity to dehydrogenation products if the lattice oxygen plays an important role in the

reaction. If the metal-oxygen bond is strong (as shown, e.g., by the reduction potential or by the heat of reoxidation), it is difficult to remove oxygen from the lattice to form oxygen-containing products, and therefore the selectivity to C_4 dehydrogenation products is high.

In this way, activity and selectivity of an oxide in selective oxidation reactions are related to the reducibility of the oxide. An oxide that is too difficult to be reduced has very low activity, while one that is too easily reduced is active but non-selective. The decrease in butane conversion and the increase in selectivity for dehydrogenation over Cs modified samples could be due to increased difficulty of the catalyst to undergo redox cycles.

We, however, observed a maximum in C_4 selectivity on increasing the Cs content and such behaviour is not visible in the TPR data. A maximum in such circumstances was also found in the previously published CO_2-TPD measurements [9]. In this way, it seems that the catalytic activity for *n*-butane ODH would be related to the reducibility of catalysts and the selectivity to dehydrogenation products would depend mainly on the acid–base character of the catalyst surface. Similar results were found by Blasco et al. [13].

The kinetic studies over unpromoted and 3% Cs promoted nickel molybdate showed that the main effects resulting from Cs addition are: an increase of the activation energies; an increase of the partial order with respect to butane for C_4 products; and a decrease of this order for products of total oxidation. The order with respect to oxygen is almost always unaffected.

Carbon oxides can proceed from the deep oxidation of adsorbed butane, intermediate species or formed dehydrogenation products. The interaction of these species with the catalyst surface is weaker when basicity increases. Therefore, with the unpromoted $NiMoO_4$, they are interacting more strongly with the catalyst and can be more easily overoxidized to CO or CO_2. In this way, when the butane concentration is increased the CO_x formation increases markedly. In this sense, the undoped catalyst must exhibit a higher partial order with respect to butane for CO_x than the Cs-doped one. With the 3% Cs–$NiMoO_4$ catalyst the dehydrogenation products desorb easier from the surface due to the higher basicity and a stronger dependence on the butane partial pressure is found (cf. Table 4).

The higher E_a values for butane activation (and for all the product formation) with the Cs-doped sample is probably related with the higher resistance to reduction of this catalyst. This fact, and the observed relationship between the catalysts activity and reducibility (i.e. increasing the resistance to reduction – by increasing the Cs content – decreases the butane conversion rate), suggests that this reaction occurs through a Mars and van Krevelen mechanism [28]. Work on this topic is underway, but a detailed investigation specially concerning the interaction between gaseous oxygen and the catalyst surface is crucial.

An almost zero order with respect to oxygen was found for the oxidative dehydrogenation processes with both catalysts, which also suggests a redox-type mechanism. However, CO_x formation exhibits a positive order with respect to O_2. Therefore, the CO_x formation would also result from the attack of adsorbed hydrocarbon species by gaseous O_2. Consequently, the role of gaseous oxygen would be either to replenish the lattice oxygen consumed, reoxidizing the solid (according with the Mars and van Krevelen process), or to form CO_x by attacking the weakened C–C bonds of the adsorbed species.

Acknowledgements

L.M. Madeira thanks PRAXIS XXI Program from JNICT (Junta Nacional de Investigaçao Científica e Tecnológica) for financial support. Support of this work by the European Community (contract No. CHRX-CT92-0065) is gratefully acknowledged.

References

[1] J.L. Brito, A.L. Barbosa, A. Albornoz, F. Severino, J. Laine, Catal. Lett. 26 (1994) 329.
[2] B.C. Gates, J.R. Katzer, G.C.A. Schuit, Chemistry of Catalytic Processes, McGraw-Hill, New York, 1979, p. 390.
[3] C. Mazzocchia, R. Del Rosso, P. Centola, An. Quim. 79 (1983) 108.
[4] U. Ozkan, G.L.J. Schrader, J. Catal. 95 (1985) 137.
[5] U. Ozkan, G.L.J. Schrader, J. Catal. 95 (1985) 147.
[6] C. Mazzocchia, C. Aboumrad, C. Diagne, E. Tempesti, J.M. Herrmann, G. Thomas, Catal. Lett. 10 (1991) 181.

[7] C. Mazzocchia, A. Kaddouri, R. Anouchinsky, M. Sautel, G. Thomas, Solid State Ionics, 63–65 (1993) 731.
[8] R.M. Martin-Aranda, M.F. Portela, L.M. Madeira, F. Freire, M. Oliveira, Appl. Catal. A 127 (1995) 201.
[9] F. J Maldonado-Hódar, L.M. Madeira, M.F. Portela, R.M. Martín-Aranda, F. Freire, J. Mol. Catal. A 111 (1996) 313.
[10] L. Owens, H.H. Kung, J. Catal. 148 (1994) 587.
[11] M.A. Chaar, D. Patel, M.C. Kung, H.H. Kung, J. Catal. 105 (1987) 483.
[12] D. Patel, P.J. Andersen, H.H. Kung, J. Catal. 125 (1990) 132.
[13] T. Blasco, J.M. López Nieto, A. Dejoz, M.I. Vázquez, J. Catal. 157 (1995) 271.
[14] J.L. Brito, J. Laine, K.C. Pratt, J. Mater. Sci. 24 (1989) 425.
[15] F. Di Renzo, C. Mazzocchia, G. Thomas, A.M. Vernay, React. Sol. 6 (1988) 145.
[16] M.A. Tsurov, P.V. Afanasiev, V.V. Lunin, Appl. Catal. A 105 (1993) 205.
[17] L.M. Madeira, F.J. Maldonado-Hódar, M.F. Portela, F. Freire, R.M. Martin-Aranda, M. Oliveira, Appl. Catal. A 135 (1996) 137.
[18] M.A. Kipnis, D.A. Agievskii, Kinet. Katal. 22 (1981) 1252.
[19] A.I. Vagin, N.V. Burmistrova, V.I. Erofeev, React. Kinet. Catal. Lett. 28 (1985) 47.
[20] K.A. Samigov, Study of the phase composition, structure, and nature of active centers in alumina–nickel–molybdenum hydrodesulfurization catalysts, Author's Abstract of Candidate's Dissertation, Tashkent State University, Tashkent, 1973.
[21] T.S. Ismailov, G.Sh. Talipov, N.Sh. Inoyatov, Catalytic Processing of Hydrocarbon Feedstocks, No. 5, Tashkent, 1971, p. 91.
[22] G.A. Tsigdinos, W.W. Swanson, Ind. Eng. Chem. Prod. Res. Dev. 17 (1978) 208.
[23] S.A. Driscoll, D.K. Gardner, U.S. Ozkan, J. Catal. 147 (1994) 379.
[24] C. Fourgeaud, A. Fuchs, Statistique (Collection Universitaire de Mathématiques, 24), Dunod, Paris, 1967, Chap. 6.
[25] I.M. Chakravarti, R.G. Laha, J. Roy, Handbook of Methods of Applied Statistics, Vol. I, John Wiley and Sons, New York, 1967, Chap. 5–6.
[26] C. Martin, V. Rive, A. Gonzalez-Elyse, J. Catal. 114 (1988) 473.
[27] H.H. Kung, in D.D. Eley, H. Pines, W.O. Haag (Eds.), Advances in Catalysis, Vol. 40, Academic Press, New York, 1994, p. 1.
[28] P. Mars, D.W. van Krevelen, Chem. Eng. Sci. (Spec. Suppl.) 3 (1954) 41.